

# Quench and Stability Modelling of a Metal-Insulation Multi-Double-Pancake High-Temperature-Superconducting Coil

Andrew V. Gavrilin<sup>✉</sup>, Dylan J. Kolb-Bond, Kwang Lok Kim<sup>✉</sup>, Kwangmin Kim, William S. Marshall<sup>✉</sup>, and Iain R. Dixon<sup>✉</sup>

**Abstract**—The most detailed, first-principle simulation model of a quench in a high-temperature superconducting metal-insulation multi-module/multi-double-pancake coil, wound with a REBCO coated superconductor/tape and normal-metal tape (co-wind), was developed. It enables one to simulate a normal zone propagation, or non-propagation, in the subtle multi-turn structure of the coil's pancakes due to the inductive coupling and transverse electric contact between all the REBCO turns and co-wind turns along with the external circuit and active and passive quench protection systems. In doing so, the multi-module coil's structure is represented as a “rectilinear equivalent” electric circuit, a branched multi-decker multi-rectangle planar grid, which facilitates the mathematical formulation, using the standard electric circuit differential equations and the Kirchhoff's rules. The transient non-linear comprehensive heat conduction equations are employed to model the thermal part of the phenomenon at the same level of detail. All this turns the model into an effective design tool for metal-insulated, -stabilized and/or -reinforced multi-module coils. A parametric study of quench in a 6-module no-insulation (NI) test coil, using a stainless-steel thin co-wind, was conducted to identify the possibilities of the model. The profound effect of the transverse contact resistivity on an NI-coil quench behavior is confirmed and detailed.

**Index Terms**—No-insulation REBCO coils, first-principle model, quench, stability, computer simulation, contact resistance.

## I. INTRODUCTION

THE DEVELOPMENT of so-called metal-insulated (metal-insulation) HTS magnets that have become popular in recent years requires professionally justified, high-precision and efficient tools for computer analysis of the processes which govern those magnets' operation. Such coils, which seem to be the most practical “subspecies” of so-called no-insulation (NI) coils, are usually assembled from double-pancakes/modules “two-in-hand”-wound with a REBCO coated conductor/tape and normal-metal tape, “a co-wind”, which is typically a highly resistive one. Modeling the quench behavior is a problem of

Manuscript received November 29, 2020; revised March 2, 2021 and March 10, 2021; accepted March 12, 2021. Date of publication March 17, 2021; date of current version May 6, 2021. This work supported in part by National High Magnetic Field Laboratory and in part by National Science Foundation under Cooperative Agreements DMR-1644779 and DMR-1839796, and the State of Florida. (Corresponding author: Andrew V. Gavrilin.)

The authors are with National High Magnetic Field Laboratory, Tallahassee, FL 32310 USA (e-mail: gavrilin@magnet.fsu.edu).

Color versions of one or more figures in this article are available at <https://doi.org/10.1109/TASC.2021.3066548>.

Digital Object Identifier 10.1109/TASC.2021.3066548

particular complexity, which is much more sophisticated than that of an insulation coil wound with the same REBCO tape and insulated co-wind as reinforcement and is not even fully understood yet. To be specific, in the analysis of a quench, the most difficult part is modelling the process of redistribution of the stored energy in the winding due to the inductive coupling between the turns and the transverse/radial currents through the co-wind.

The first models of quench in NI-coils, where the transverse/radial currents are allowed, were those with lumped parameters, i.e., rather simplistic e.g., [1]–[5]. The underlying assumption of such models is that the transverse/radial resistance of a NI-pancake, the main component of which is the contact resistance, works as a parallel shunt resistance with respect to the conductor that gains “the azimuthal resistance” [2] in the event of a quench. At best, an advanced version of such a lumped-parameter model [3], [4], extended to a multi-pancake coil, could track/simulate the axial/pancake-to-pancake quench propagation qualitatively, but hardly quantitatively, which could be no longer enough at the current level of NI-technology.

A breakthrough can be considered the creation of a more advanced model [6], [7], based on the above-mentioned “old textbook” assumption, that simulates both the axial/pancake-to-pancake and radial quench propagation in a multi-module NI-coil: using this model, various quench behaviors were predicted and some important new features of the process of a quench itself were identified. However, two “self-evident” assumptions, used as the basis of the model, can somehow limit its generality, which can lead to the dependence of the calculation accuracy on the analyzed situation and turn out to be somewhat different for different coils. Such assumptions are (a) grouping the turns into relatively thick radial sections within the pancakes and again (b) assigning the transverse/contact resistance to the shunt resistance of such a radial section (that carries circumferentially the transport current). The latter makes the equivalent electric circuit of a NI-coil's internal structure identical to that of a highly sectioned LTS winding [6], [7], i.e., by and large, streamlines it. This is an elegant and often efficient, but still somewhat simplified and thus hardly universal, approach, as we explain below. However, the tremendous advantage of the model is a relatively short computational time, which is extremely important if one needs to do many estimation calculations when developing a user magnet.

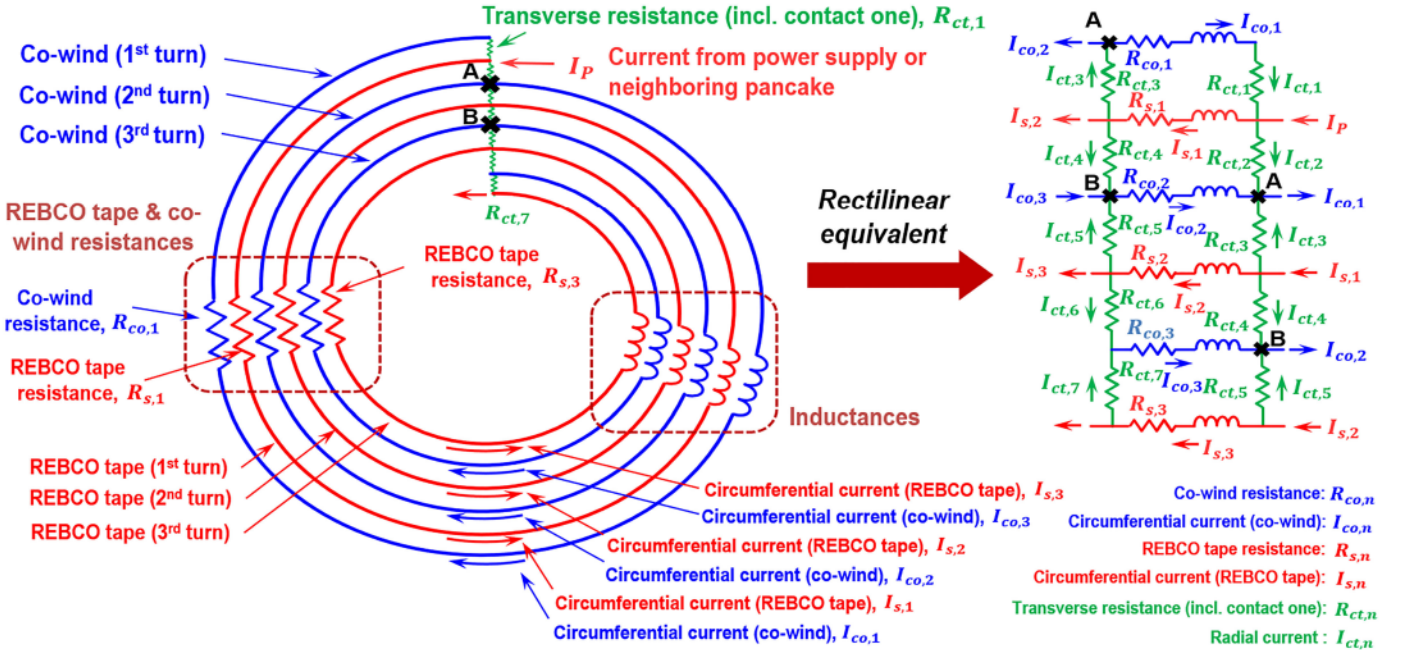


Fig. 1. A 3-turn fragment of equivalent electric circuit of a REBCO-tape-wound pancake (left) and its “rectilinear equivalent” (right) that facilitates the mathematical formulation of the model. The spatial increment is the radius-dependent length of a turn.

A different approach, based on the idea of using the most detailed equivalent electric circuit (“distributed network” and/or PEEC models) of the spiral structure of a pancake and employing the Kirchhoff’s rules, without omitting or simplifying anything, was tried in some works, e.g., [5], [8]–[11]. However, the simulations in these works were limited to literally a single pancake, while an elegant attempt to extend this approach to a multi-pancake coil [12] was associated, as we see, with the use of noticeable simplifications of the analytical unit cell that led to the simpler equations, respectively, the validity and applicability of which we do not undertake to evaluate here. The goal of our work is to develop and extend the PEEC/“distributed network” approach to a multi-module coil without simplifying anything or missing out on details (which, to the best of our knowledge, has not been done before), and so that the model has the potential to be applied to a multi-coil system. Such a task is trivially complicated by the fact that even to imagine and depict the equivalent electric circuit of a multi-spiral system, which is actually a 3D one, is very difficult, and not just to depict, but to depict so that using the diagram it becomes possible to formulate the circuit governing equations. To eliminate this difficulty, a new way of depicting the equivalent circuit was proposed: “a rectilinear equivalent” or “a multi-rectangle planar grid”.

## II. A NEW FORM OF EQUIVALENT ELECTRIC CIRCUIT OF A METAL-INSULATION MULTI-MODULE COIL

The concept of a “rectilinear equivalent” of spiral electric circuit of a pancake’s structure is detailed in Fig. 1: it is to abandon the spiral network and move to the equivalent rectilinear one. As can be inferred from the diagram, new features not considered before in publications [5]–[11] are added in order to be able to deal with the most general case: the resistance in the circumferential direction and inductance of the co-wind.

The transverse resistance, the main component of which can turn out to be the contact resistance between the conductor and co-wind, is included in its most general form. The rectilinear (“straightened”) equivalent has a familiar, convenient visual appearance and thus makes it much easier and unmistakable to apply the electric circuit ordinary differential equations and the Kirchhoff’s rules to formulate the model equations.

Even in the relatively simple case of a single-module coil, using such “a rectilinear equivalent”, which turns into a multi-rectangle planar grid (Fig. 2), instead of the perplexing double-spiral network, seems to be the easiest way to come up with formulation of the model equations. Moreover, in the case of a multi-module coil (Fig. 3), to employ the planar grid seems to be the only way to enable the mathematical formulation. As can be seen in Fig. 2, the numbering is different from that in Fig. 1: Turn 1 is the innermost turn of each pancake in Figs. 2 & 3 that is the standard numbering used in the model as well as the notation. The neighboring double-pancakes (Fig. 3) are connected at the coil’s outer diameter (OD), whereas two pancakes within each double-pancake are connected at the inner diameter (ID) through a transition turn they share (Figs. 2 & 3). The inlet and outlet (terminals) are located at the OD;  $I_0$  is the coil current which is damped by the transverse and azimuthal/circumferential resistances of the conductor and co-wind turns and/or an external dump resistance, if any, in the event of a quench.

The only real simplification, which is not fundamental, is the spatial increment size equal to the radius-dependent length of a turn. In the case of a multi-pancake coil with a large number of turns per pancake, this simplification becomes a very minor one. Indeed, in this case, even if a quench occurs locally, on a small part of one turn, the big picture of the quench development depends little on the initial condition due to the round cylinder geometry of the coil [9]–[11], that is to say, in the quench simulation, the disturbance may be modelled as occurring on the

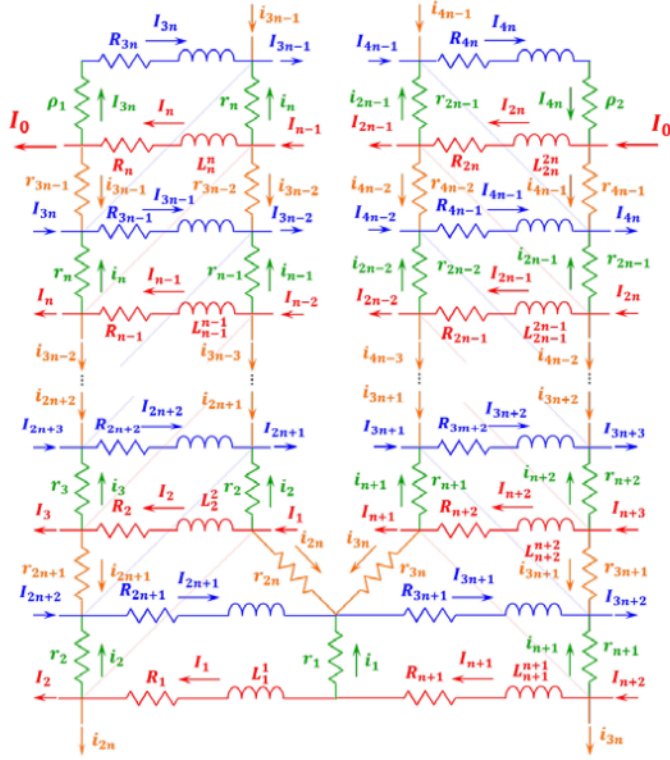


Fig. 2. A multi-rectangle planar grid as an equivalent electric circuit of a double-pancake coil structure; 'n' REBCO turns and 'n' co-wind turns per pancake.

whole turn. Nonetheless, the model has the potential to reduce the increment size if required, e.g., if it becomes necessary to account for the contact resistance inhomogeneity along the conductor within a turn (the contact sporadicity). The approach is also applicable in the case of non-circular configuration. If applied so, the increment size must be chosen accordingly.

### III. THE MODEL GOVERNING CIRCUIT EQUATIONS

#### A. Single Double-Pancake Equivalent Circuit Equations

To show what equations of the equivalent network are obtained using the above approach and to explain the opening possibilities, it seems to be best to use the example of a single double-pancake coil (Fig. 2). In this case,  $m = 2$ , i.e., we have only two pancakes connected at the ID, and there are  $2n$  REBCO turns and  $2n$  co-wind turns totally in the coil, respectively.

For the innermost REBCO turns,  $j = 1$  and  $n + 1$ ,  $k = \text{int}[j/n]$ , the system of circuit equations is:

$$\begin{aligned} \sum_{i=1}^{4n} (L_{ji} \dot{I}_i + I_j (R_j + r_{j-n-k} + r_{(k+2)n})) \\ = (I_{j+2n} + I_0) \cdot r_{(k+2)n} + I_{j+(-1)^k n} \cdot r_{j-n-k} . \end{aligned} \quad (1)$$

For other REBCO turns,  $1 < j \leq n$  and  $n + 1 < j \leq 2n$ ,  $l = j + 2n - 1$ , we have:

$$\sum_{i=1}^{4n} (L_{ji} + L_{li}) \dot{I}_i + I_j (R_j + r_l)$$

$$= (I_{j-1} - I_0) r_{l-1} + (I_{l+1} + I_0) r_l - I_l (R_l + r_{l-1}) , \quad (2)$$

For the co-wind innermost turns, the equations are obtained in the following form:

$$\begin{aligned} \sum_{i=1}^{4n} (L_{ji} + L_{1i}) i_i + I_j (R_j + r_2) = (I_2 - I_0) r_2 + I_{n+1} r_1 \\ - I_1 (R_1 + r_1) , \text{ for Pancake 1 (left), } j = 2n + 1 , \end{aligned} \quad (3)$$

$$\begin{aligned} \sum_{i=1}^{4n} (L_{ji} + L_{n+1} i) \dot{I}_i + I_j (R_j + r_{n+1}) \\ = (I_{n+2} - I_0) r_{n+1} + I_1 r_1 - I_{n+1} (R_{n+1} + r_1) , \\ \text{for Pancake 2 (right), } j = 3n + 1 , \end{aligned} \quad (4)$$

For the co-wind outmost turns, we get:

$$\begin{aligned} \sum_{i=1}^{4n} (L_{ji} + L_{n i}) \dot{I}_i + I_j (R_j + \rho_1) = (I_{j-1} + I_0) r_n \\ - I_n (R_n + r_n) , \text{ for Pancake 1, } j = 3n , \text{ and} \end{aligned} \quad (5)$$

$$\begin{aligned} \sum_{i=1}^{4n} (L_{ji} + L_{2n} i) \dot{I}_i + I_j (R_j + \rho_2) = (I_{j-1} + I_0) r_{2n-1} \\ - I_{2n} (R_{2n} + r_{2n-1}) , \text{ for Pancake 2, } j = 4n , \end{aligned} \quad (6)$$

For the regular/inner co-wind turns, the compact form of the equations is as follows:

$$\begin{aligned} \sum_{i=1}^{4n} (L_{ji} + L_{\varsigma i}) \dot{I}_i + I_j (R_j + r_{\varsigma+3-k}) \\ = (I_{\varsigma+3-k+\xi} - I_0) r_{\varsigma+3-k} + (I_{j-1} + I_0) r_{\varsigma+2-k} \\ - I_{\varsigma+3-k} (R_{\varsigma+2-k+\xi} + r_{\varsigma+2-k}) , \\ \varsigma = j - 2n , \\ \xi = \begin{cases} 0, & 2n + 1 < j < 3n \\ 1, & 3n + 1 < j < 4n \end{cases} \end{aligned} \quad (7)$$

In the equations, here and below, the circumferential currents,  $I_j$ , and Ohmic resistances,  $R_j$ , of the turns refer to the conductor, if  $j \leq m \cdot n$ , and to the co-wind, if  $j > m \cdot n$ . The transverse resistance,  $r_j$ , is that between a conductor turn and the overlying co-wind turn, if  $1 \leq j < m \cdot n$ , and the underlying co-wind turn, if  $j \geq m \cdot n$ . The "terminal" resistances,  $\rho_1$  and  $\rho_2$ , enable modeling specific conditions at the inlet and outlet, whereas  $L$  is the  $2m \cdot n$  by  $2m \cdot n$  inductance matrix. The inductances are calculated as such for closed circular loops instead of spiral turns that is a minor simplification due to the extremely small thickness of REBCO tape and co-wind, however, a more accurate model can be employed if necessary.

It is noteworthy that the polarity of the circumferential currents,  $I_j$ , in the REBCO turns and co-wind turns is specially chosen to be the same (within each analytical unit cell) (Figs. 2 & 3) so that the inductances in (2-7) are added and not subtracted, which makes the matrix of the summed inductances seamlessly invertible. The transverse resistance,  $r_j$ , includes the resistance

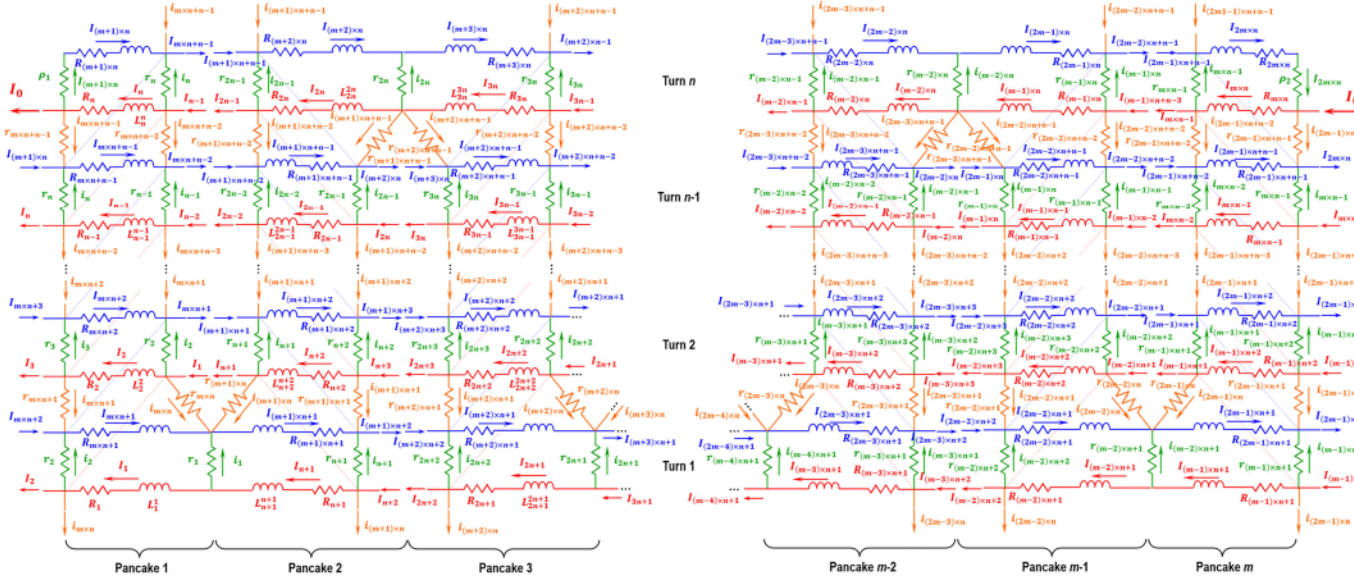


Fig. 3. A multi-rectangle planar grid as an equivalent electric circuit of a multi-module metal-insulation coil's subtle structure, i.e., with alternating REBCO-tape and normal-metal co-wind turns; 'm' pancakes totally with 'n' REBCO turns and 'n' co-wind turns per pancake.

of the contact and the co-wind resistance in the radial direction. All the resistances in the model are dependent on the temperature and/or any other characteristic, if necessary (see also below at the end of section B).

Calculating the radial currents is a straightforward task:

$$i_j = \begin{cases} i_j = I_{n+1} - I_1, & j = 1 \\ i_j = I_0 - I_j + I_{j+2n-1}, & 1 < j \leq n \\ i_j = \begin{cases} -(I_0 - I_{j+1} + I_{j+2n}), & n < j < 2n \\ -(I_0 - I_{j-2n+1} + I_{j+1}), & 2n \leq j < 3n \\ I_0 - I_{j-2n+1} + I_{j+1}, & 3n \leq j < 4n. \end{cases} & \end{cases} \quad (8)$$

It is almost obvious that the applicability of the model is not limited to the co-wind material, which allows us to consider its various types: stainless-steel, Hastelloy, bronze, etc. for NI-pancake-wound coils.

If necessary, although this is perhaps an unusual application, the model can be employed even for some insulation coils. For instance, the model enables us to simulate a quench in an insulation coil "three-in-hand" wound with (a) a REBCO tape, (b) copper tape ("extra copper co-wind") or another REBCO tape, and (c) insulated metallic reinforcement (e.g., a sol-gel plated stainless steel strip [13]). In this case, the "underlying" radial currents must be set equal to zero, or the "underlying" transverse resistances must be set extremely high instead. The insulated steel reinforcement should be excluded from the multi-rectangle planar grid as its individual component carrying a circumferential current, because such a current can be an induced current only in nature, due to the inductive coupling alone, and so it may be assumed to be vanishingly small.

Regardless, the main application of this approach is, of course, for NI-coils two-in-hand-wound with a co-wind that has a much higher electric resistivity than that of the copper matrix of the REBCO tape.

## B. A Highly-Resistive-Metal-Insulation Multi-Module Coil. Simplified Equivalent Circuit Equations.

As noted above, a multi-module REBCO-tape-wound NI-coil typically uses a highly resistive material such as stainless steel as the co-wind. Numerous comparative analyses showed clearly that in this case, the system of circuit differential equations may be greatly simplified "with impunity": its dimension may be halved by excluding the co-wind inductance, however, not making any other changes in the electric circuit pattern (Fig. 3) is vital.

Thus, for the innermost REBCO turns,  $k = \text{int}[j/n]$ , the system of circuit equations in the compact form is:

$$\sum_{i=1}^{m \cdot n} L_{ji} \dot{I}_i + I_j (R_j + r_{j-v \cdot n}) = (I_{j+1} - I_0) r_{j+1-v} + I_{j+(-1)^v n} r_{j-v \cdot n} - I_{j+m \cdot n} (R_{j+m \cdot n} + r_{j+1-v}), \quad (9)$$

$$v = \begin{cases} 0, & \text{when } k \text{ is even} \\ 1, & \text{when } k \text{ is odd} \end{cases}.$$

For the outermost REBCO turns, the equations, (10–13), are as follows.

Pancake 1 (the left end pancake):

$$\sum_{i=1}^{m \cdot n} L_{ji} \dot{I}_i + I_j (R_j + r_j) = (I_{j+m \cdot n-1} + I_0) r_j - I_{j+m \cdot n} (R_{j+m \cdot n} + \rho_1). \quad (10)$$

Pancake 'm' (the right end pancake):

$$\sum_{i=1}^{m \cdot n} L_{ji} \dot{I}_i + I_j (R_j + r_{j-1}) = (I_{j+m \cdot n-1} + I_0) r_{j-1} - I_{j+m \cdot n} (R_{j+m \cdot n} + \rho_2). \quad (11)$$

Inner pancakes with odd index numbers, i.e., 3, 5, ...,  $m - 1$ :

$$\sum_{i=1}^{m-n} L_{ji} \dot{I}_i + I_j (R_j + r_j) = (I_{j+m-n-1} + I_0) r_j - I_{j+m-n} (R_{j+m-n} + r_{j-n}) + I_{j+(m-1)\cdot n} r_{j-n}. \quad (12)$$

Inner pancakes with even index numbers, i.e., 2, 4, ...,  $m - 2$ :

$$\sum_{(i=1)}^{m-n} L_{ji} \dot{I}_i + I_j (R_j + r_j) = (I_{j+m-n-1} + I_0) r_{j-1} - I_{j+m-n} (R_{j+m-n} + r_j) + I_{j+(m+1)\cdot n} r_j. \quad (13)$$

Finally, the equations for the other, inner/regular REBCO turns (in all pancakes) are:

$$\sum_{i=1}^{m-n} L_{ji} \dot{I}_i + I_j (R_j + r_{j-v}) = (I_{j+1} - I_0) r_{j+1-v} + (I_{j+m-n-1} + I_0) r_{j-v} - I_{j+m-n} (R_{j+m-n} + r_{j+1-v}). \quad (14)$$

Having calculated the circumferential currents in the conductor turns, it is not difficult to calculate the circumferential currents in the co-wind and then the radial currents using the Kirchhoff's rules.

Let us consider the case when the solution of the above equations satisfies the following conditions:

$$\max |I_j - I_0| \ll |I_0| \text{ and} \quad (15)$$

$$|I_{j+m-n}| \ll |I_0|, j = 1, \dots, m \cdot n. \quad (16)$$

If so, then (14) can be transformed to this form:

$$\sum_{i=1}^{m-n} L_{ji} \dot{I}_i + I_j (R_j + r_{j-v}) \cong I_0 r_{j-v}. \quad (17)$$

Equations (10)-(13), as well as the most general equations (2), take on the same form, which is nothing more than the system of circuit equations for a sectioned winding, in which each conductor "section" (with resistance  $R_j$ ) is protected by a parallel shunt resistance ( $r_j$ ), which is the transverse, that is, mainly contact, resistance, which is the underlying assumption of models like [3], [4], [6], [7]. In other words, we may reasonably assert that the transverse resistance,  $r_j$ , serves as a parallel shunt resistance for the REBCO conductor only in cases where the transverse resistance is fairly high, i.e., where the circumferential currents in the REBCO conductor do not experience significant local rises and falls, but decay with the total current of the circuit,  $I_0$ . Thus, inequalities (15,16) are the conditions for the applicability of models like [6], [7] and also a makeshift benchmark for users of lumped-parameter models from [1]–[5], [9].

Situations in which this is the case, i.e., in which conditions (15,16) are satisfied with an acceptable margin of error, are possible, if not common. However, that high "threshold" value of the transverse/contact resistance is not fixed and is difficult to determine a-priori: it changes with a change in the dimensions and other parameters of the coil, and also strongly depends on the features of the simulated event of a quench, i.e., it may

be different at different stages of the quench development. By experience from comparative analyses, with the inner diameter of a NI-coil of about 100 mm and a large number of modules in it, such a threshold value, in terms of electric contact resistivity, is at least not lower than  $10 \text{ m}\Omega \text{ cm}^2$  per contact (at the initial stage of a quench initiated by a local heat disturbance, it may turn out to be higher), but this value is given solely for orientation and is not in any way universal.

It is worth noting that on the outermost turns, the transverse resistance actually behaves just like the shunt resistance (parallel to the conductor) in any case scenario, because in (10)-(13) for these turns, there is no "unwanted" first term (that contains the current in the REBCO conductor) on the right side of those equations, but only the second and third terms (containing the co-wind currents), and inequality (16) is always satisfied. In other words, the "self-evident" assumption (used in the simplified models like [6], [7]) is always 100% justified only in relation to a single-turn pancake, where it apparently came from, and when moving to a pancake with a larger number of turns, the applicability of such models becomes limited.

The thermal part of the problem is solved at the same, if not even higher, level of detail [14], [15], in the quasi-3D approximation, taking into account all thinkable nonlinearities and transients, including the multi-stage superconducting-normal transition mode [14], [15] and the critical current dependence on the local values of temperature, magnetic field magnitude and angle [16], which spatial distributions are updated at each time step of the numerical solution finite-difference scheme. The magnetic field vector on each turn is calculated as the superposition of magnetic fields from all turns. However, effects related to the screening currents are not included yet.

#### IV. QUENCH MODELLING IN A MULTI-MODULE NI-TEST-COIL

This model, embodied in a Fortran script, is used to find out the quench characteristics of NI test coils, thereby contributing to a better planning of such quench tests. Particularly, a parametric study of the process of a local unprotected quench development in a 6-module NI-coil (named Petten Test Coil 3, PTC3, after the outer Petten LTS magnet, which provides a background magnetic field up to 6.6 T) was performed (at 4.2K). The coil assembly image is given in Fig. 4. PTC3 with the bore radius of 50 mm has 53 turns per pancake wound with a non-graded 4.1 mm wide SuperPower REBCO tape; the co-wind is a  $12.7 \mu\text{m}$  thick bare stainless-steel tape. The OD approximates 109 mm. Two pancakes within each module are separated by a 0.25 mm thick G-10 insulation, whereas the inter-module G-10 spacer thickness is 1.08 mm that impedes the spread of heat axially. The initial current is taken equal to 400 A that results in the maximum total field of 13.3T in PTC3, before a quench starts, and the maximum critical current fraction of 36% (in the end pancakes), respectively. The thermal contact resistance is taken equal to  $10^{-5} \text{ m}^2 \text{ K/W}$  (the same everywhere).

In the simulations, the electric contact resistivity ranged from  $0.05 \text{ m}\Omega \text{ cm}^2$  per contact, i.e.,  $0.1 \text{ m}\Omega \text{ cm}^2$  per turn, to start with, to  $6 \text{ m}\Omega \text{ cm}^2$  per contact that is  $12 \text{ m}\Omega \text{ cm}^2$  per turn. The latter is close to the average value measured before quench tests began. We presumed that the contact resistivity is the same

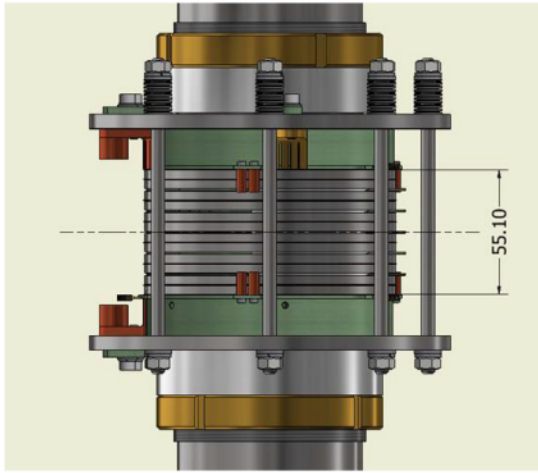


Fig. 4. Petten Test Coil 3 (PTC3) assembly. Side view.

for all contacts between the conductor and co-wind, i.e., along the entire length of the tape within each pancake, and fixed (a time-variable contact resistivity can easily be included, but the variability is not known yet to the extent required).

In the case of relatively low contact resistivity ( $0.1 \text{ m}\Omega \text{ cm}^2$  per turn) to initiate a quench locally, even in one of the end pancakes, is difficult, so a strong temperature disturbance, 104.2 K throughout the entire pancake 1, was used (Fig. 5). Even if initiated, by instantly normalizing the entire pancake 1, the quench develops very slowly and the coil current is hardly attenuated, bypassing Module 1 radially through the very low contact resistance, for a noticeable period of time that is followed by a kind of electromagnetic avalanche (Fig. 5), which is a rapid, albeit sequential, shockwave quenching of all other pancakes that causes an almost instantaneous damping of the coil current.

The quench within each pancake is typically a sequential normalization of its turns with the preceding surge of the circumferential current in each of them (this process in pancake 7 is shown as an illustration in Fig. 6). In fairness, it should be noted that such a shockwave quench development in a multi-module NI-coil as one of possible forms of the quench behavior was first predicted using the semi-empirical model [6], [7], albeit for somewhat different parameters.

With increasing contact resistivity, the probability of an electromagnetic avalanche becomes small. Moreover, the self-protection mechanism turns on, which impedes the quench development (Fig. 7). In this case of contact resistivity of  $12 \text{ m}\Omega \text{ cm}^2$  per turn, a local quench (initiated by means of a 50 ms long very strong pulse of current in a stray heater attached to the entire side surface of pancake 1) cannot pass the central high critical current area of the coil, and only pancakes 1 and 2, and a very small fraction of pancake 3 as well, turn out to be normalized. As a result, the coil current decays slowly: the time constant exceeds 0.4 s that would look like an incredibly long duration if PTC3 was an insulation coil, all other things being equal. It should be noted that, in contrast to the previous case of low resistivity, in this case, the “jumps” in the circumferential currents on the REBCO turns are relatively small. The most significant ones are observed in pancake 2 (the neighbor of the

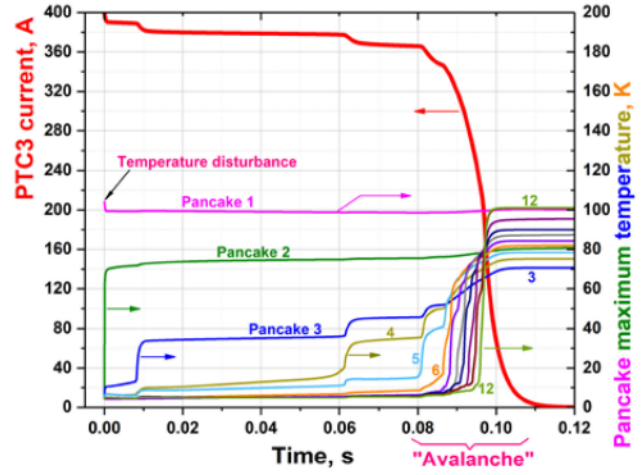


Fig. 5. PTC3 circuit current and maximum temperature in the coil's pancakes in the event of an unprotected quench in the form of electromagnetic avalanche. Contact resistivity of  $0.1 \text{ m}\Omega \text{ cm}^2$  per turn. No external dump resistance. Power supply is off.

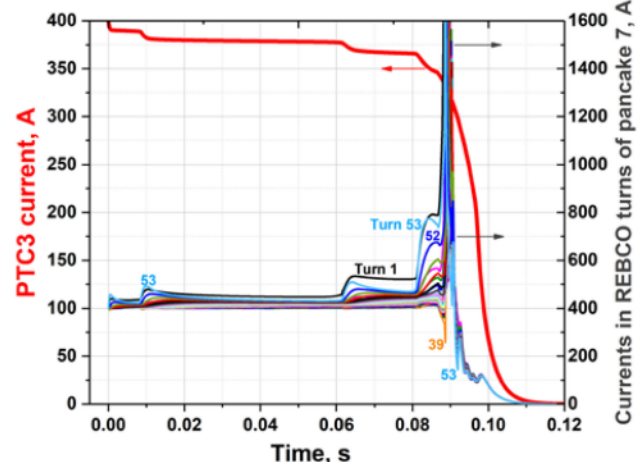


Fig. 6. Transient leaps of the circumferential current in the REBCO turns of pancake 7 in the event of an electromagnetic avalanche. Contact resistivity of  $0.1 \text{ m}\Omega \text{ cm}^2$  per turn. No external dump resistance. Power supply is off.

heater-quenched pancake 1), where the rise is less than half of the initial current, the radial currents rise accordingly (Fig. 8), whereas in the following pancakes, no jumps are observed at all: the circumferential currents in the REBCO turns simply fade along with the current of the coil, and the radial currents do not exceed 100 A, which is 25% of the coil initial current.

It might seem logical to assume that at intermediate values of the contact resistivity ( $\sim 1 \text{ m}\Omega \text{ cm}^2$  per turn) the time constant value of the PTC3 current decaying process in the event of a local quench should also turn out to be intermediate, i.e., between the ultra-short one at the electromagnetic avalanche and that at the high resistivity of  $12 \text{ m}\Omega \text{ cm}^2$ . However, such an assumption would be wrong: the contact resistance intermediate in value, on the one hand, turns out to be insufficiently small to lead to a shockwave quench development, and, on the other hand, it is too small for the process of damping the coil current to be fast, and so the time constant can reach several seconds. This “snail” mode of an NI-coil current decaying is never observed, if an appropriate external dump resistance is employed promptly.

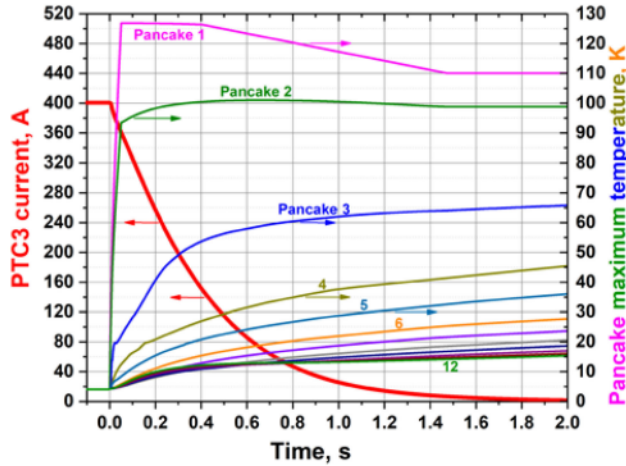


Fig. 7. PTC3 circuit current and maximum temperature in the coil's pancakes in the event of an unprotected quench. Contact resistivity of  $12 \text{ m}\Omega \text{ cm}^2$  per turn. No external dump resistance. Power supply is off.

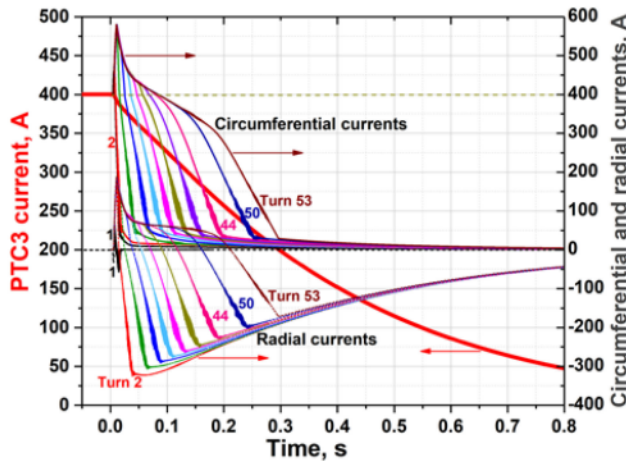


Fig. 8. The transient circumferential currents in the REBCO turns and radial currents in pancake 2 in the event of an unprotected quench. The transients are shown selectively. Contact resistivity of  $12 \text{ m}\Omega \text{ cm}^2$  per turn. No external dump resistance. Power supply is off.

## V. CONCLUSION

A new technique for creating comprehensive simulation models of a quench in a HTS multi-double-pancake NI-coil wound with a REBCO coated conductor has been proposed, based on the use of an equivalent electrical circuit which includes practically all thinkable components and features. The validity of the methodology has been proven using a precise analytical method, which also made it possible to assess the applicability of well-known and widely used approximate models. The effectiveness of the approach was demonstrated using the example of a 6-module test coil.

## ACKNOWLEDGMENT

The authors would like to thank W. D. Markiewicz, T. A. Painter, and J. Lu for numerous fruitful discussions, M. D. Bird and H. Bai for unflagging support and interest to this work,

critical remarks and timely raised issues, and S. T. Bole for the test coil drawing. The first author A. V. Gavrilin is grateful to A. Akhmeteli for constructive and guiding criticism of the mathematical formulation and various valuable comments.

## REFERENCES

- [1] A. V. Dudarev *et al.*, "Superconducting windings with 'short-circuited' turns," in *Proc. Inst. Phys. Conf. Ser. 158*, IOP Publishing Ltd. (EUCAS'97 Proc.), 1997, pp. 1615–1618.
- [2] S. Hahn, D. K. Park, J. Bascuñán, and Y. Iwasa, "HTS pancake coils without turn-to-turn insulation," *IEEE Trans. Appl. Supercond.*, vol. 21, no. 3, pp. 1592–1595, Jun. 2011.
- [3] K. R. Bhattacharai *et al.*, "Understanding quench in no-insulation (NI) REBCO magnets through experiments and simulations," *Supercond. Sci. Technol.*, vol. 33, 2020, Art. no. 035002.
- [4] K. Kim *et al.*, "Design and performance estimation of a 20 T 46 mm no-insulation all-REBCO user magnet," *IEEE Trans. Appl. Supercond.*, vol. 30, no. 4, Jun. 2020, Art. no. 4602205.
- [5] S. Noguchi, "Electromagnetic, thermal, and mechanical quench simulation of NI REBCO pancake coils for high magnetic field generation," *IEEE Trans. Appl. Supercond.*, vol. 29, no. 5, Aug. 2019, Art. no. 4602607.
- [6] W. D. Markiewicz, T. A. Painter, I. R. Dixon, and M. D. Bird, "Quench transient current and quench propagation limit in pancake wound REBCO coils as a function of contact resistance, critical current, and coil size," *Supercond. Sci. Technol.*, vol. 32, no. 10, pp. 105010–105023, 2020.
- [7] W. D. Markiewicz, J. J. Jaroszynski, D. V. Abraimov, R. E. Joyner, and A. Khan, "Quench analysis of pancake wound REBCO coils with low resistance between turns," *Supercond. Sci. Technol.*, vol. 29, no. 2, 2016, Art. no. 025001.
- [8] T. Wang *et al.*, "Analyses of transient behaviors of no-insulation REBCO pancake coils during sudden discharging and overcurrent," *IEEE Trans. Appl. Supercond.*, vol. 25, no. 3, Jun. 2015, Art. no. 4603409.
- [9] W.-K. Chan, F. Scurti, and J. Schwartz, "Mechanisms to enhance stability, post-quench recovery and availability in non-insulated REBCO magnets," in *Proc. 25th Int. Conf. Magnet Technol. (MT-25 Conf.)*, Amsterdam, The Netherlands, Aug./Sep., 2017, [Online]. Available: [https://indico.cern.ch/event/445667/contributions/2562795/attachments/1514916/2363781/Or09-02\\_WanKan\\_MT-25\\_Amsterdam\\_2017\\_v2\\_FS.pdf](https://indico.cern.ch/event/445667/contributions/2562795/attachments/1514916/2363781/Or09-02_WanKan_MT-25_Amsterdam_2017_v2_FS.pdf). Accessed on: Nov. 17, 2020.
- [10] Y. Wang, W.-K. Chan, and J. Schwartz, "Self-protection mechanisms in no-insulation (RE) $\text{Ba}_2\text{Cu}_3\text{O}_x$  high temperature superconductor pancake coils," *Supercond. Sci. Technol.*, vol. 29, no. 4, 2016, Art. no. 045007.
- [11] W.-K. Chan and J. Schwartz, "Improved stability, magnetic field preservation and recovery speed in (RE) $\text{Ba}_2\text{Cu}_3\text{O}_x$ -based no-insulation magnets via a graded-resistance approach," *Supercond. Sci. Technol.*, vol. 30, no. 7, Jun. 2016, Art. no. 074007.
- [12] R. Miyao, H. Igarashi, A. Ishiyama, and S. Noguchi, "Thermal and electromagnetic simulation of multistacked no-insulation REBCO pancake coils on normal-state transition by PEEC method," *IEEE Trans. Appl. Supercond.*, vol. 28, no. 3, Apr. 2018, Art. no. 4601405.
- [13] H. Kandel *et al.*, "Sol-gel-derived  $\text{Al}_2\text{O}_3$ – $\text{SiO}_2$  composite coating for electrical insulation in HTS magnet technology," *IEEE Trans. Appl. Supercond.*, vol. 22, no. 5, Oct. 2012, Art. no. 7701605.
- [14] A. V. Gavrilin *et al.*, "Comprehensive quench analysis of the NHMFL 32T all-superconducting magnet system," in *CHATS On Applied Superconductivity*, Univ. Bologna, Bologna, Italy, Sep. 14–16, 2015, [Online]. Available: [https://indico.cern.ch/event/372812/contributions/1792178/attachments/1158596/1667005/19\\_Gavrilin.pdf](https://indico.cern.ch/event/372812/contributions/1792178/attachments/1158596/1667005/19_Gavrilin.pdf). Accessed on: Nov. 17, 2020.
- [15] A. V. Gavrilin and H. W. Weijers, "Comprehensive modelling study of quench behaviour of the NHMFL 32 T all-superconducting magnet system. Input data and methodology aspects," in *Proc. 5th Int. Workshop Numer. Modelling High Temp. Superconductors ("HTS Modelling 2016")*, Bologna, Italy, Jun. 15–17, 2016, [Online]. Available: <http://www.die.ing.unibo.it/pers/morandi/didattica/Temporary-HTSModelling2016/Gavrilin.pdf>. Accessed on: Nov. 17, 2020.
- [16] D. K. Hilton, A. V. Gavrilin, and U. P. Trociewitz, "Practical fit functions for transport critical current versus field magnitude and angle data from (RE)BCO coated conductors at fixed low temperatures and in high magnetic fields," *Supercond. Sci. Technol.*, vol. 28, no. 7, 2015, Art. no. 04002.